Differences of Skin Movement Artifacts During Loaded and Unloaded Cycling Exercises on the Thigh and Shank Using 3D Fluoroscopy

Jia-Da Li[1], Mei-Ying Kuo[2], Tung-Wu Lu[1,3*], Tsung-Chi Lin[1], Yu-Huan Wu[1], Horng-Chaung Hsu[4]

[1]Institute of Biomedical Engineering, National Taiwan University, Taipei, Taiwan, R.O.C.
[2]Department of Physical Therapy, China Medical University, Taiwan, R.O.C.
[3]Department of Orthopaedic Surgery, School of Medicine, National Taiwan University, Taiwan, R.O.C.
[4]Department of Orthopaedics, China Medical University Hospital, Taichung, Taiwan, R.O.C.

Abstract—**Contributions of muscle contraction to the displacement of skin markers relative to the underlying bone are unclear. The study integrated a CT-to-bi-plane fluoroscopy method and the stereophotogrammetric system to obtain accurate kinematics of the femur and tibia, and quantify the soft tissue artifacts (STA) of the thigh and shank during cycling with and without resistance. Thigh markers were found to have less consistent STA patterns between loading conditions than the shank markers, especially the markers attached on the mid-thigh. Markers close to joint centers showed more anterior and proximal displacements during loaded cycling.**

Keywords—**Soft tissue artifacts; Cycling; Muscle contraction; Loading conditions.**

I. Introduction

Displacements of skin markers relative to the underlying bone, called soft tissue artifacts (STA), are considered related to the angular displacements of the adjacent joint, especially for markers close to the joint. For markers away from the joint, muscle contraction may contribute more to the observed STA. However, the roles played by these two factors in the STA of the thigh and shank markers have not been clearly identified in vivo. During cycling exercise the lower extremities form a close loop mechanism with the frame and crank/pedaling system of the bicycle, generating highly repeatable motions. This provides a good opportunity to study the changes of the patterns of the STA under minimum and strong contractions of the muscles. The current study aimed to compare the changes of the soft tissue artifacts (STA) of the thigh and shank markers during cycling with and without resistance by measuring accurately the kinematics of the femur and tibia using a CT-to-bi-plane fluoroscopy method and stereophotogrammetric system.

II. Matrial and methods

Subjects

Five healthy young adults (age: 20.8±0.6 years, height: 171.6±2.5 cm, mass: 61.4±7.3 kg) participated in the current study with informed written consent as approved by the Institutional Research Board. All subjects were free of neuromusculoskeletal dysfunction.

Experimental procedure

Each subject wore 10 skin markers on the medial and lateral femoral epicondyles (LFE and MFE), medial, anterior, and lateral side of mid-thigh (THIM, THIC, THIL), tibial tuberosity (TT), fibular head (FH), anterior side of mid-shank on the tibia (SHAC), and medial and lateral malleolus (MMA, LMA). They performed stationary cycling in two conditions: null resistance and an average resistance of 20 Nm. The 3D marker trajectories were measured using a 12-camera motion capture system at a sampling rate of 120Hz (Vicon Motion Systems Ltd., UK). The knee was imaged simultaneously at 60 Hz by a bi-plane dynamic fluoroscopy system (ALLURA XPER FD, Philips). The knees of the subjects were also CT scanned and used to construct CT-based bone models. A subject static calibration was also performed. A metronome was used to keep cycling speed at 30 RPM, which gave about 120 fluoroscopic images per cycle (approximate 3° crank angle per frame) and 240 data points for stereophotogrammetric system.

Data analysis

The subject-specific, CT-based bone models were registered to the fluoroscopy images using a volumetric model-based fluoroscopy-to-CT registration method [1], giving poses of the femur and tibia, and the knee joint center positions. The means and standard deviations of the bone pose errors were less than -0.4 (0.4) mm and -0.5° (0.3°) for all translational and all angular components, respectively [1]. During subject calibration without skin movement, bone coordinate systems were defined for the thigh and shank based on the registered poses of the femur and tibia following the ISB convention, which coincided with the segment-embedded coordinate systems. Meanwhile, the position of a skin marker relative to the associated bone coordinate system was taken as the reference for STA calculation. During movement, given the measured marker coordinates relative to the stereophotogrammetry coordinate system, the components of the STA in the bone coordinate system at time t, corresponding to the anterior/posterior (A/P), proximal/distal (P/D) and medial/lateral (M/L) components, were calculated as the current position of the marker relative to the bone and fluoroscopy coordinate systems, respectively. The gold standard positions of these markers, i.e., those of the so-called virtual bone markers (VBM), in the fluoroscopy coordinate system were obtained.

Statistical Analysis

Descriptive statistics of the results were obtained, namely ensemble-averaged marker displacements, maximum and minimum marker displacements, as well as the maximum difference (MaxD) and root mean squared differences (RMSD) of the marker displacements between loaded and unloaded pedaling conditions. Between-condition comparisons were performed using paired t-tests for all the above variables.

III. Results

Accurate 3D skeletal kinematics of the knee during cycling was measured so that accurate skin marker movement patterns between loaded and unloaded pedaling were obtained. Increased resistance during cycling also increased the demand of muscle contractions in order to keep up to the specified cycling speed, with only subtle changes in the joint angles in response to different loading conditions.

Compared to the null resistance condition, the thigh markers were affected more than the shank markers under loaded condition (Fig 1, Tables 1 & 2). Overall the averaged RMSD between the two conditions were 2.87 mm for the thigh markers and 2.16 mm for the shank ones, respectively. LFE and MFE were mostly affected in the A/P direction, followed by P/D direction (Table 1). MFE showed the most anterior displacement relative to the underlying bone during loaded condition. THIL and THIM were the most sensitive markers during resistance condition, with the biggest changes in the A/P direction followed by M/L direction. During loaded condition, THIC and THIM showed significantly more anterior and lateral displacements.

In contrast to the thigh markers, the shank markers demonstrated more consistent movement patterns between loaded and unloaded conditions, except for the LMA and MMA in the A/P direction and M/L direction (Table 2). TT and SHAC were mostly affected in the M/L direction, and FH in the A/P direction. During loaded condition, FH and SHAC were found to show significantly increased proximal displacements.

IV. Discussion

The current study aimed to compare the changes of the soft tissue artifacts (STA) of the thigh and shank markers during cycling with and without resistance. During cycling as a close loop motion, the knee flexion angles were similar between the two loading conditions. As expected, the markers on the thigh were affected more by the cycling resistance, and thus muscle contractions, than the shank markers, especially the markers on the mid-thigh in the A/P direction.

Although the shank markers were less affected by the loading conditions, the markers close to the ankle joint (i.e. LMA and MMA) were found to have less consistency in the A/P and M/L direction. This could be attributed to the changes of the ankle joint motion in response to the increased pedal reaction forces. One the other hand, the lateral and medial malleoli were of convex surfaces, so their positions relative to underlying bone were sensitive to the angular displacement of the ankle.

V. Conclusion

In conclusion, the current study showed that markers did not follow consistent movement patterns in specific directions when subject to different cycling resistances. This was considered primarily a result of the differences in the muscle contractions in response to the loading conditions, which should be considered in future development of subject-specific STA compensation methods.

VI. Acknowledgment

The authors gratefully acknowledge financial support from Nation Science Council, Taipei, Taiwan (NSC 103-2627-B-039-001-)

VII. References

1. Lin, C.-C., Lu, T.-W. et al. (2013) Comparisons of Surface vs. Volumetric Model-Based Registration Methods Using Single-Plane vs. Bi-Plane Fluoroscopy in Measuring Spinal Kinematics. Med Eng Phys, 1350-4533.

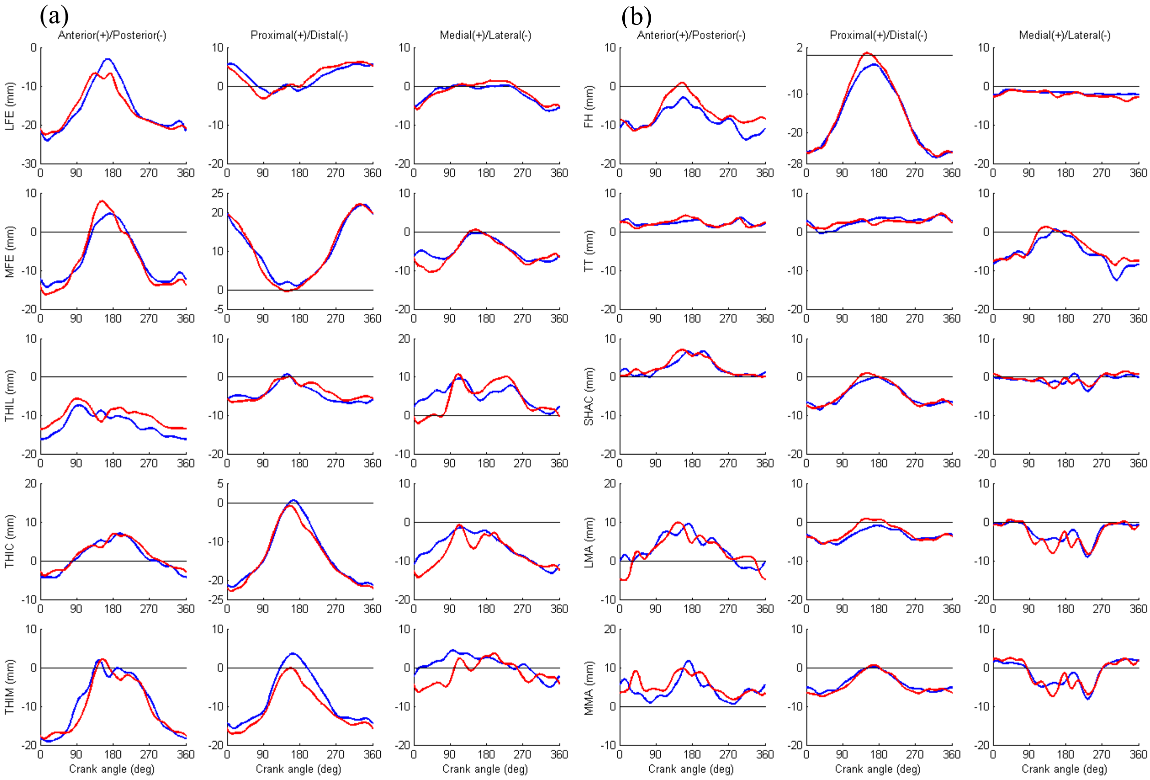

Figure 1. The STA of a typical subject: (a) thigh and (b) shank markers during cycling with null resistance (blue line) and resistant (red line). The crank angle of 0° was defined as the pedal was at the top position.

Table 1. The STA of the thigh markers: means (SD) of ensemble-averaged displacement, maximum and minimum displacements, as well as the maximum difference (MaxD) and root mean squared differences (RMSD) of the thigh markers relative to the underlying bone between loaded and unloaded pedaling in the anterior(+)/posterior(-) (A/P), proximal(+)/distal(-) (P/D) and medial(+)/lateral(-) (M/L) directions of the bone coordinate system. An asterisk indicates significant difference between loaded and unloaded condition.

Thigh		**Mean**		**Maximum**		**Minimum**		**MaxD**	**RMSD**
(mm)		0 Nm	20 Nm	0 Nm	20 Nm	0 Nm	20 Nm		
LFE	A/P	-11.3 (3.9)	-11.8 (3.2)	0.0 (3.1)	-0.4 (3.3)	-18.9 (5.2)	-19.7 (4.1)	5.6 (0.5)	2.7 (0.5)
	P/D	-0.9 (2.2)	-0.4 (2.7)	3.1 (2.3)	4.1 (3.6)	-5.5 (2.0)	-5.4 (1.7)	3.5 (0.6)	1.7 (0.4)
	M/L	-2.8 (1.5)	-2.3 (1.7)	-0.6 (1.4)	0.2 (2.1)	-7.0 (1.3)	-5.8 (1.8)	3.3 (1.8)	1.3 (0.5)
MFE	A/P	-16.5 (6.3)	-15.3 (6.0)	-3.3 (6.0)*	-0.5 (5.7)*	-24.7 (6.8)	-24.9 (6.6)	6.0 (1.2)	2.7 (0.6)
	P/D	7.6 (2.9)	7.8 (2.9)	18.5 (4.0)	20.2 (3.7)	-1.0 (1.4)	-1.6 (1.0)	4.9 (3.3)	1.9 (1.1)
	M/L	-6.3 (3.0)	-6.1 (2.7)	-0.8 (2.1)	0.1 (1.6)	-10.6 (3.8)	-11.1 (3.3)	3.4 (1.6)	1.3 (0.5)
THIL	A/P	-2.3 (7.9)	-1.8 (6.8)	4.6 (8.1)	6.0 (8.0)	-10.0 (8.5)	-8.3 (5.7)	12.9 (9.2)	5.1 (2.5)
	P/D	-6.4 (2.9)	-6.3 (3.6)	-1.1 (2.3)	-0.6 (2.5)	-9.7 (3.5)	-10.7 (4.9)	4.2 (1.3)	1.8 (0.4)
	M/L	0.2 (3.1)	-0.6 (3.0)	4.6 (4.2)	4.0 (4.4)	-3.4 (2.0)*	-5.8 (2.4)*	6.2 (1.7)	3.0 (0.6)
THIC	A/P	-2.6 (2.7)*	-1.1 (2.6)*	2.4 (3.2)	3.6 (3.9)	-7.0 (2.4)	-5.3 (2.9)	7.2 (4.9)	3.0 (1.5)
	P/D	-14.4 (0.9)	-15.0 (0.6)	-4.6 (3.7)	-4.5 (3.7)	-20.4 (1.9)	-24.2 (4.5)	6.2 (4.3)	2.3 (1.3)
	M/L	4.1 (8.3)*	1.3 (6.9)*	9.3 (8.5)	6.6 (6.0)	-1.1 (8.1)	-2.9 (7.8)	7.3 (2.7)	3.6 (1.6)
THIM	A/P	-19.9 (8.3)*	-16.1 (6.8)*	-5.5 (6.7)	-4.5 (5.3)	-32.8 (10.0)*	-28.7 (9.2)*	15.8 (7.4)	6.6 (2.5)
	P/D	-7.6 (5.5)	-7.9 (5.1)	-1.1 (5.7)	-1.9 (5.8)	-11.9 (5.8)	-12.8 (4.9)	4.8 (1.5)	2.1 (0.5)
	M/L	3.1 (7.3)*	0.7 (6.3)*	8.9 (7.1)	7.3 (6.1)	-2.0 (7.4)*	-4.7 (7.5)*	7.4 (1.8)	3.8 (0.8)